ELSEVIER

Journal of Fluids and Structures 22 (2006) 713–719

JOURNAL OF FLUIDS AND STRUCTURES

www.elsevier.com/locate/jfs

Brief communication

# Comparing numerical and analytical solutions for squeeze-film levitation force

A. Minikes, I. Bucher*

*Dynamic Laboratory, Faculty of Mechanical Engineering, Technion—Israel Institute of Technology, Haifa 32000, Israel*

Received 11 November 2004; accepted 9 February 2006
Available online 4 May 2006

**Abstract**

In this paper, a two-dimensional numerical study on the levitation force induced by pressure radiation in a gas squeeze film is carried out. In particular, the validity of the pressure release boundary condition and the isothermal assumptions are examined by a CFD scheme. The results are compared to a one-dimensional analytical solution, leading to findings on the role and accuracy of commonly used boundary conditions. It appears that when taking into consideration the energy leakage near the edges of the levitated object, the levitation force due to the squeeze film could be smaller by up to 50% in comparison with the analytical, one-dimensional solution that assumes pressure release conditions.


*Keywords:* Squeeze film; Radiation pressure; Reynolds equation; Nonlinear acoustics

## 1. Introduction

In mechanical systems where a gas squeeze-film is generated, the forces induced by the film may have a crucial influence on the dynamic performance of the systems (Bao, 2000; Gross, 1962; Bhushan, 1999). Such an influence is not restricted to energy dissipation, i.e. to damping effects and to drag forces, but it also affects pressure radiation which creates a constant levitation force and a spring-like behavior, in this case. Mechanical systems where a gas is present between two close surfaces exhibiting high frequency normal vibrations are commonly found in micromechanical devices (Bao, 2000) and in levitation systems (Salbu, 1964; Hashimoto et al., 1996; Nomura et al., 2002; Minikes and Bucher, 2003).

While the damping force and drag force exerted by the squeeze film are dealt with in the literature (Bao, 2000; Gross, 1962; Bhushan, 1999), the levitation force induced by radiation pressure in the squeeze film is rarely considered. Radiation pressure becomes significant for small scale devices such as in micromechanical (MEMS) applications. Normal oscillating excitation between two planar surfaces can create forces to the extent that second-order effects become significant, and the generated gas film has a time-averaged pressure larger than the surrounding. Under fast vibrations, the viscous flow cannot be instantaneously squeezed; consequently, compressibility forces reach equilibrium with viscous forces.

*Corresponding author. Tel.: 972 4 8293153; fax: 972 4 8295711.
*E-mail address:* bucher@technion.ac.il (I. Bucher).

0889-9746/$ - see front matter 
doi:10.1016/j.jfluidstructs.2006.02.004

The existing analytical approaches for the levitation phenomenon are based on either conventional acoustic radiation, where the fluid is assumed inviscid or on a variant of the Reynolds equation that incorporates viscous effects. Hashimoto et al. (1996) provided a simplified mathematical formulation by which the levitation force is based on the acoustic radiation theory; Chu and Apfel (1982) have demonstrated this effect in a simplified, one-dimensional case. Nomura et al. (2002), presented a numerical analysis of a two-dimensional axisymmetric pressure field, solving the continuity and momentum equations for adiabatic conditions. The disagreement between the numerical results (Nomura et al., 2002) and the analytical solution (Hashimoto et al., 1996) was attributed to energy leakage in the peripheries of the levitated object; not accounted for by the one-dimensional model.

The present work, examines the validity of the Reynolds equation for the prediction of the squeeze film levitation. A two-dimensional CFD analysis, similar to that presented by Nomura et al. (2002), was carried out, taking into account not only the influence of the near-field radiation pressure in the peripheries of the levitated object but also the influence of the temperature filed. The numerical results are compared with an analytical second-order solution of the Reynolds equation derived by means of perturbation technique with pressure release boundary conditions.

## 2. Problem description

Consider the case illustrated in Fig. 1 where a symmetric half of a flat wall having a width $L$ and a much larger length, is placed at a mean distance $Z$ from a flat vibrating plane. The distance $Z$ is of order $10^{-4}$ m and is two orders of magnitude smaller than the width $L$. The driving surface oscillates in the normal direction at a frequency $\omega$ (order of $10^5$ rad/s) and amplitude $\varepsilon Z$ ($\varepsilon \ll 1$)· The vibrating surface squeezes the gas that occupies the clearance between the planes, generating a time averaged pressure higher than the surrounding.

The gas flow in a cross section (a two-dimensional flow) is governed by the compressible and viscous Navier-Stokes equations. Introducing the following dimensionless variables where the dimensional variables are denoted by a tilde:

$$x=\frac{\tilde{x}}{L},\quad y=\frac{\tilde{y}}{Z},\quad t=\omega\tilde{t},\quad u=\frac{\tilde{u}}{c_0},\quad v=\frac{\tilde{v}}{c_0},\quad \mu=\frac{\tilde{\mu}}{\mu_0},$$
$$\rho=\frac{\tilde{\rho}}{\rho_0},\quad T=\frac{\tilde{T}}{T_0},\quad p=\frac{\tilde{p}}{\rho_0 c_0^2},\quad e=\frac{\tilde{e}}{c_0^2};$$

here, $x$ and $y$ are the space coordinates, $t$ represents time, $u$ and $v$ are the flow velocities in the $x$ and $y$ direction, respectively. The gas viscosity and density are denoted by $\mu$ and $\rho$, respectively, $T$ is temperature, $p$ stands for pressure and $e$ the gas internal energy state. The subscript 0 in the variables designates the quantities at initial conditions of the gas which was chosen to be standard atmospheric air, and $c_0$ stands for the speed of sound. The Navier-Stokes equations in Cartesian coordinates can be written in the compact dimensionless form (Tannehill et al., 1997):

$$\frac{\partial U}{\partial t}+\frac{\partial E}{\partial x}-\frac{\partial G}{\partial x}+\frac{\partial F}{\partial y}-\frac{\partial W}{\partial y}=0, \tag{1}$$

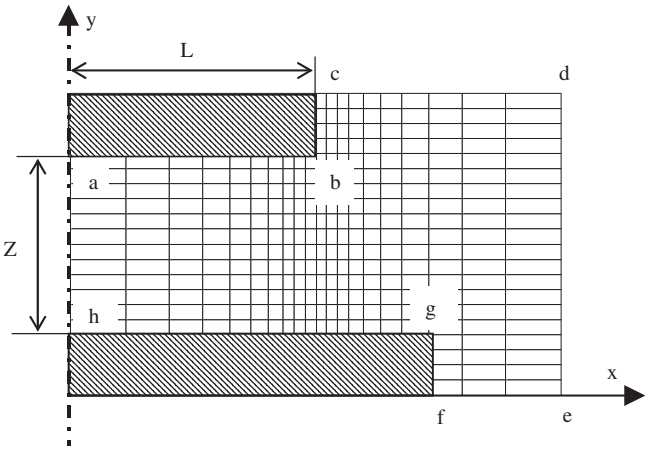


Fig. 1. Schematic layout of half of the symmetric of the problem.

where $U$, $E$, $G$, $F$ and $W$ are the vectors

$$U=\begin{Bmatrix}\rho\\ \rho u\\ \rho v\\ E_t\end{Bmatrix},\quad E=\frac{1}{kL}\begin{Bmatrix}\rho u\\ \rho u^2+p\\ \rho uv\\ (E_t+p)u\end{Bmatrix},\quad G=\frac{1}{kL}\begin{Bmatrix}0\\ \tau_{xx}\\ \tau_{xy}\\ u\tau_{xx}+v\tau_{xy}+q_x\end{Bmatrix},$$

$$F=\frac{1}{kZ}\begin{Bmatrix}\rho v\\ \rho vu\\ \rho v^2+p\\ (E_t+p)v\end{Bmatrix},\quad W=\frac{1}{kL}\begin{Bmatrix}0\\ \tau_{xy}\\ \tau_{yy}\\ v\tau_{yy}+u\tau_{xy}+q_y\end{Bmatrix};$$

in these vectors, $k=\omega/c_0$ is the wave number and $E_t$ represents the total energy density, $E_t=\rho[e+(u^2+v^2)/2]$. The components of the shear-stress tensor and heat flux vector in dimensionless form are given by

$$\tau_{xy}=\frac{\mu}{\mathrm{Re}_z}\left(\frac{\partial u}{\partial y}+\frac{Z}{L}\frac{\partial v}{\partial x}\right),\quad \tau_{xx}=\frac{2}{3}\frac{\mu}{\mathrm{Re}_z}\left(2\frac{Z}{L}\frac{\partial u}{\partial x}-\frac{\partial v}{\partial y}\right),\quad \tau_{yy}=\frac{2}{3}\frac{\mu}{\mathrm{Re}_z}\left(2\frac{\partial v}{\partial y}-\frac{Z}{L}\frac{\partial u}{\partial x}\right),$$
$$q_x=\frac{\mu}{(\gamma-1)\mathrm{Pr}\times\mathrm{Re}_z}\frac{Z}{L}\frac{\partial T}{\partial x},\quad q_y=\frac{\mu}{(\gamma-1)\mathrm{Pr}\times\mathrm{Re}_z}\frac{\partial T}{\partial y}. \tag{2}$$

The Reynolds number is $\mathrm{Re}_z=\rho_0 c_0 Z/\mu_0$ and Sutherland's formulae for viscosity and thermal conductivity ($\kappa$) were applied: $\mu=(T_0+110.4)T^{3/2}/(T_0T+110.4)$, $\kappa=C_p\mu/\mathrm{Pr}$, where $C_p$ is the specific heat at constant pressure, and Pr is the Prandtl number (taken as constant). Since the problem involves relatively low temperatures (room temperatures), air is considered a calorically perfect gas and a specific heat ratio of $\gamma=1.4$ is taken for the following relations: $e=T/\gamma(\gamma-1)$, $p=\rho T/\gamma$. The time averaged force ($W$) per unit length acting on the upper wall is expressed by integrating the normal component of the stress tensor along the wall width and averaging over a time period at a steady state conditions:

$$W=\frac{1}{2\pi}\int_0^{2\pi}\int_0^{L}\left[-p+\frac{2}{3}\frac{\mu}{\mathrm{Re}_z}\left(2\frac{\partial v}{\partial y}-\frac{Z}{L}\frac{\partial u}{\partial x}\right)\right]_{y=Z}\hat{n}\,\mathrm{d}x\,\mathrm{d}t, \tag{3}$$

where $W$ is normalized by $\rho_0 c_0^2 L$ and $\hat{n}$ is an outward unit vector normal to the surface. The $x$ derivative vanishes due the symmetry in the problem. Taking into consideration the ambient pressure outside the wall, the time-averaged levitation force becomes

$$W=\frac{1}{2\pi}\int_0^{2\pi}\int_0^{L}\left[p-\frac{1}{\gamma}-\frac{4}{3}\frac{\mu}{\mathrm{Re}_z}\left(\frac{\partial v}{\partial y}\right)_{y=Z}\right]\mathrm{d}x\,\mathrm{d}t. \tag{4}$$

### 2.1. Boundary conditions—numerical model

In order to solve the Navier-Stokes equations subjected to initial and boundary conditions, a numerical computation method has been applied. A half of the symmetric integration domain is shown schematically in Fig. 1. The upper and lower rectangles represent the levitated plate and the vibrating surface, respectively. In practice, the levitated plate vibrates in response to the pressure fluctuations in the gas film. According to experimental observations, obtained by Nomura et al. (2002) and by Minikes and Bucher (2003), these vibrations are two to three orders of magnitude smaller than the vibration amplitude of the driving surface; therefore, the levitated plate can be adequately modeled as a stationary wall. Utilizing a no-slip wall boundary condition along the boundaries a–b and b–c where the flow velocities vanish, gives: $u|_{\mathrm{a-b}}=u|_{\mathrm{b-c}}=0$, $v|_{\mathrm{a-b}}=v|_{\mathrm{b-c}}=0$.

The small amplitude vibrations of the exciting surface can be represented as a kinematical boundary-constraint hence, the flow velocities on the boundaries of the driving surface vibrating harmonically are: $u|_{\mathrm{f-g}}=u|_{\mathrm{g-h}}=0$, $v|_{\mathrm{f-g}}=0$, $v|_{\mathrm{g-h}}=V\times\sin(t)$. Where $V=\varepsilon\omega Z/c_0$ is the dimensionless velocity amplitude.

On the outer boundary lines of the integration domain, lines c–d–e–f, nonreflecting boundary conditions were adopted according to Thompson (1987) and Poinsot and Lele (1992). The location of these boundaries was determined by an iteration process in which the boundaries are placed far enough from the gas film to neglect the shear-stresses and heat flux on these boundaries, and to prevent numerical oscillations of the solution. For the sake of improving the

accuracy of the scheme, a logarithmic grid stretching of the $x$-axis was carried out as illustrated schematically in Fig. 1. The transformation forms an evenly spaced computational plane to the physical plane was accomplished through the logarithmic stretching used by Holst (1977). This time-dependent system was solved by employing an explicit numerical computation method similar to that employed by Nomura et al. (2002): an explicit MacCormak finite difference scheme suggested by Turkel (1980) with fourth-order accuracy in space and second-order accuracy in time. The computational domain is typically divided into 60 grids along the $y$-axis and 400 grids along the $x$-axis. The computational grid was refined until a difference smaller than 1% between two subsequent solutions of the levitation force was observed. The stability of the scheme was ensured by satisfying the Courant-Friedrichs-Lewy condition for numerical convergence (Tannehill et al., 1997).

### 2.2. Approximate analytical solution

The Reynolds equations are derived by performing an order-of-magnitude analysis on the governing equations. This analysis reveals that the pressure gradient in the normal direction can be neglected (Langlois, 1962). Integrating the continuity equation across the film thickness and substituting the velocity profile into the momentum equation in the $x$ direction results in the governing one-dimensional, time-dependent Reynolds equation for laminar, Newtonian, isothermal (the isothermal assumption will be discussed later on), and compressible thin film flow (Langlois, 1962):

$$\frac{\partial}{\partial x}\left(z^3 p \frac{\partial p}{\partial x}\right) = \sigma \frac{\partial}{\partial t}(pz), \quad p(x, t=0) = 0, \quad p(x = \pm 0.5, t) = 0, \tag{5}$$

where $z = \tilde{z}/Z$, is the normalized mean clearance between the surfaces, and the dimensionless squeeze number is defined as: $\sigma = (12\omega\mu_0 L)/(\rho_0 c_0^2 Z^2)$; pressure release conditions were used at the edges.

When solving the Reynolds equation for the pressure radiation in the film, a second-order solution, accounting for nonlinear effects should be considered. It is assumed that the deviation from the ambient pressure is expanded up to order $\varepsilon^2$ terms as follows:

$$p(x, t) = 1 + \varepsilon \Pi_A(x, t) + \varepsilon^2 \Pi_B(x, t) + \mathcal{O}(\varepsilon^3). \tag{6}$$

Substituting this equation together with the prescribed time variation of the clearance between the surfaces $H(t) = 1 + \varepsilon\cos(t)$ into Eq. (6) creates linear differential equations that can be solved (Minikes et al., 2004) , to obtain the pressure and consequently the levitation force:

$$W = \frac{1}{2\pi}\int_0^{2\pi}\int_{-1/2}^{1/2}\left(p - \frac{1}{\gamma}\right)\Big|_{y=Z} \mathrm{d}x\,\mathrm{d}t = \frac{5\varepsilon^2}{4\beta}\left[\frac{\beta\cos(\beta) + \beta\cosh(\beta) - \sinh(\beta) - \sin(\beta)}{\cos(\beta) + \cosh(\beta)}\right]; \tag{7}$$

here $\beta = \sqrt{\sigma/2}$.

Eq. (7) shows that the normalized time averaged levitation force is proportional to the square of the excitation amplitude for a given squeeze number. For vibration amplitudes, up to about one third of the mean clearance ($\varepsilon \leqslant 0.3$), this second-order perturbation solution is in good agreement with a numerical solution of the Reynolds equation (Minikes et al., 2004).

## 3. Results

The assumptions of pressure release on the boundaries and an isothermal behavior of the film are necessary for deriving the Reynolds equation and in order to obtain the solution for the levitation. The comparisons presented in this section focus on examining the adequacy of these assumptions.

### 3.1. The assumption of pressure release boundary condition

The influence of the surface dimensions on the levitation force was examined in order to assess their influence on the correct choice of boundary conditions. When the driving surface is larger than the levitated pressure the assumption of pressure release at the boundaries should be considered with caution. As mentioned before, the Reynolds equation does not incorporate pressure gradients in the normal direction to the vibrating surfaces ($y$-axis); therefore, near-field acoustic pressure created by the exposed portion of the driving surface is not accounted. The eddy acoustic streaming near the boundaries is varying periodically with time, influencing the pressure gradients in the squeezed gas layer. Fig. 2 presents some numerical results of the levitation force, computed with the numerical CFD scheme as function of the

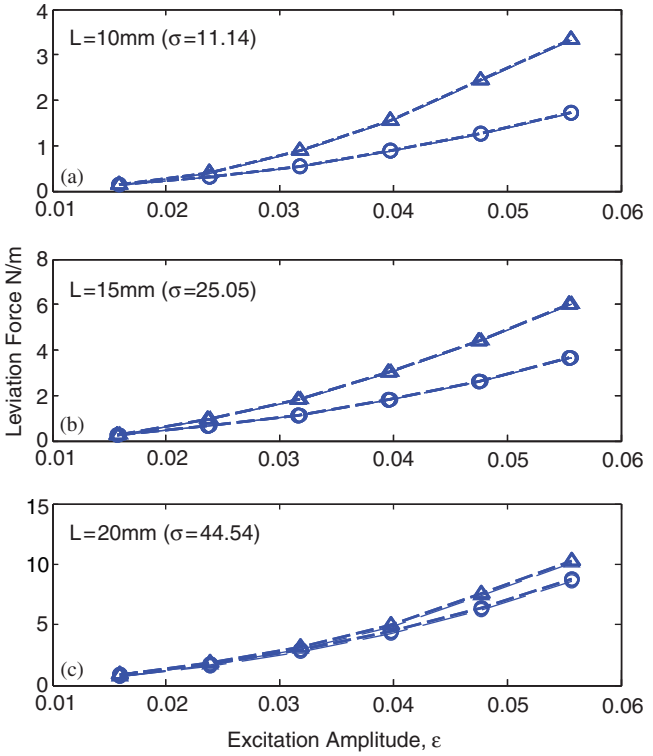


Fig. 2. Numerical results of the levitation force as function of the excitation amplitude for two cases: (i) lines (g–h) = (a–b) in Fig 1 (triangles); (ii) lines (g–h) = 1.2(a–b) in Fig 1 (circles).

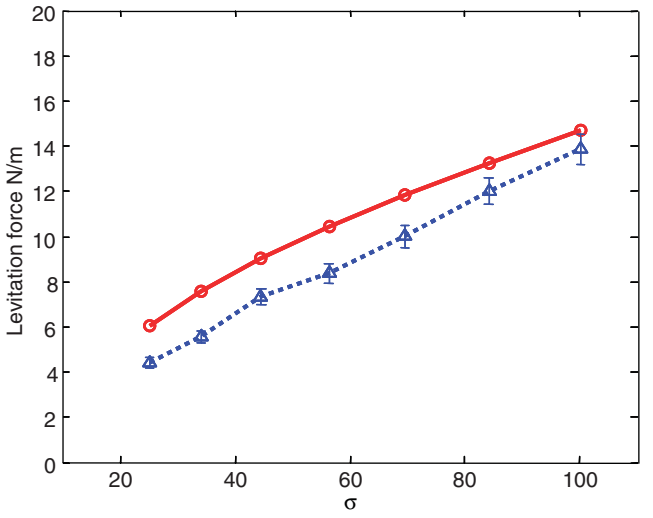


Fig. 3. Levitation force as function of the squeeze number: Analytical solution, Eq. (15) (circles) and numerical solution (triangles, ±5% error bar).

excitation amplitude for different levitated surface sizes, $L = 10$, 15, 20 (or squeeze numbers $\sigma = 11.14$, 25.05, 44.54, respectively). The excitation amplitudes did not exceed $\varepsilon \leqslant 0.0557$, limiting the local error to 5.6%. The triangles in Fig. 2 indicate the levitation force when both surfaces are of the same size (line a–b is equal to line g–h in Fig. 1) and the circles indicate the levitation force when the driving surface (line g–h in Fig. 1) is larger by 20% than the levitated

surface (line a–b in Fig. 1). The physical values of parameters used in the numerical computations are: $\omega = 2\pi * 20 \times 10^3\,\mathrm{rad/s}$, $\mu_0 = 1.8462 \times 10^{-5}\,\mathrm{kg/ms}$, $Z = 100\,\mu\mathrm{m}$, $\rho = 1.1774\,\mathrm{ks/m^3}$, $T_0 = 300\,\mathrm{K}$, $\mathrm{Pr} = 0.722$.

The numerical results appearing in Fig. 2 suggest that for low squeeze numbers the levitation force is significantly influenced by the near-field acoustic pressure at the boundaries. It shows that for $\sigma = 11.14$ (Fig. 2(a)) the levitation force may drop up to 50% when the vibrating surface is larger than the levitated surface. In such cases, assuming pressure release ($p = 1$) at the boundaries is inadequate. As the squeeze number increases this influence decreases as can be seen in Fig. 2(b) and (c). This behavior may be explained by examining the pressure gradients in the film. The pressure gradients in the gas layer increase with the increase of squeeze number. The larger the pressure gradients in the film are, the less sensitive they are to small variations in the pressure on the boundaries.

As the Reynolds equation was solved analytically under the assumption of pressure release at the boundaries, a comparison of the analytical solution of Eq. (7) with the numerical results could be considered adequate, only for the case of small $\sigma$ where the driving surface and the levitated surface are of the same width.

The analytical solutions indicated by circles and the numerical solutions that are presented by triangles, are compared. The local error is limited by $\pm 5\%$ as the displacement excitation amplitude was $\varepsilon = 0.0477$. The agreement between the solutions is reasonably good when considering all the assumptions made for deriving the Reynolds equation. At squeeze numbers higher than those presented in Fig. 3, the pressure gradients in the film increase to the extent that a much finer grid is necessary for depicting properly the flow properties.

### 3.2. The assumption of isothermal behavior

The characteristic time of temperature variations across the squeezed film can be approximate by $t \approx Z^2/\alpha \approx \mathcal{O}(10^{-5}\,\mathrm{s})$ where $\alpha$ is the thermal diffusivity of the gas. When dealing with excitation frequencies in the range of $\omega \approx \mathcal{O}(10^5\,\mathrm{rad/s})$, this characteristic time is an order of magnitude shorter than that of the periodic oscillation time. This implies that temperature dissipates in the flow significantly faster than the propagation of the flow matter; thus, the flow field could be considered as nearly uniform across the squeezed film during each time cycle. Furthermore, since the gas film is very thin and of low heat capacity when compared with that of the bearing surfaces, the whole fluid occupying the space between the plates could be treated as isothermal.

It is reasonable to expect differences in the results between a model assuming isothermal behavior and a model under an adiabatic behavior assumption. When deriving the Reynolds equation for isothermal polytropic flow ($p\rho^{-1} = \mathrm{const.}$), it is possible to replace $\rho$ by $p$ to obtain Eq. (5). However, when adiabatic behavior is postulated, the relation between the normalized pressure and density is $\rho = p^{1/\gamma}$. In such a case, Eq. (5) will take the form

$$\frac{\partial}{\partial x}\left(\frac{p^{1/n}Z^3}{\mu}\frac{\partial p}{\partial x}\right) = \sigma\frac{\partial}{\partial t}(p^{1/n}Z). \tag{8}$$

The flow viscosity varies with temperature, therefore it is no longer constant in the field. Inspecting the results obtained from an isothermal model, it appears that the fluctuations of the normalized pressure do not exceed 10%. In such case, the normalized density is nearly equal to the normalized pressure ($\rho = p^{1/1.4} \approx p$ since $p$ is close to 1) and Eq. (8) reduces to the isothermal Reynolds equation, Eq. (5).

As described earlier, the temperature in the numerical model was predetermined only at the boundaries of the surfaces, and a constant and uniform value was dictated allowing for heat flux to take place in the field. Elsewhere, the boundaries were imposed far enough from the squeeze-film where the thermal gradients were shown to be insignificant in the CFD analysis. Therefore, the assumption that the time-averaged temperature is nearly constant seems acceptable, and the small fluctuations suggest that postulating an isothermal behavior for deriving the analytical solution is adequate.

## 4. Conclusions

In this work, numerical and analytical solutions for the pressure radiation induced by a squeeze gas film were examined and compared. It has been shown that the assumption of pressure release at the boundaries, implied in the Reynolds equation, is inadequate in cases where the driving surface is sufficiently larger than the levitated surface. In such cases, numerical computations show that the near-field acoustic pressure created by the exposed portion of the driving surface influences the pressure gradients in the film, causing a reduction of up to 50% in the levitation force at low squeeze numbers. This influence reduces with the increase of the squeeze number and the pressure release condition provides satisfactory accuracy. A second-order analytical solution of the Reynolds equation has been briefly reviewed

and it was shown to be in good agreement with a two-dimensional CFD solution taking into account viscosity and compressibility effects. The question whether the squeezed film should be considered as isothermal or adiabatic was discussed and numerical computations showed that the film experiences only small temperature fluctuations (about 5%) with constant time-averaged temperature, suggesting an isothermal behavior.

## References

Bao, Min-Hang, 2000. Micro Mechanical Transducers: Pressure Sensors, Accelerometers, and Gyroscopes. Handbook of Sensors and Actuators, vol. 8. Elsevier Science, B.V.

Bhushan, B., 1999. Principles and Applications of Tribology. Wiley Inc.

Chu, B.T., Apfel, R.E., 1982. Acoustic radiation pressure produced by beam of sound. Journal of the Acoustical Society of America 72 (6), 1673–1687.

Gross, W.A., 1962. Gas Film Lubrication. Wiley Inc., NY.

Hashimoto, Y., Koike, Y., Ueha, S., 1996. Near-field acoustic levitation of planar specimens using flexural vibration. Journal of the Acoustical Society of America 100 (4), 2057–2061.

Holst, T.L., 1977. Numerical solution of axisymmetric boattai field with plume simulators. AIAA paper 1977-224.

Langlois, W.E., 1962. Isothermal squeeze films. Quarterly of Applied Mathematics XX (2), 131–150.

Minikes, A., Bucher, I., 2003. Coupled dynamics of squeeze-film levitated mass and vibrating piezoelectric disc—numerical analysis and experimental study. Journal of Sound and Vibration 263 (2), 241–268.

Minikes, A., Bucher, I., Haber, S., 2004. Levitation force induced by pressure radiation in gas squeeze films. Journal of the Acoustical Society of America 116 (1), 217–226.

Namoura, H., Kamakura, T., Matsuda, K., 2002. Theoretical and experimental examination of near-filed acoustic levitation. Journal of the Acoustical Society of America 111 (4), 1578–1583.

Poinsot, T.J., Lele, S.K., 1992. Boundary conditions for direct simulations of compressible viscous flows. Journal of Computational Physics 101, 104–129.

Salbu, E.O.J., 1964. Compressible squeeze films and squeeze bearings. Journal of Basic Engineering 86, 355–366.

Tannehill, J.C., Anderson, D.A., Pletcher, R.H., 1997. Computational Fluid Mechanics and Heat Transfer, Second edition, Taylor & Francis.

Thompson, K.W., 1987. Time dependent boundary conditions of hyperbolic systems. Journal of Computational Physics 68, 1–24.

Turkel, E., 1980. On the practical use of high-order methods for hyperbolic systems. Journal of Computational Physics 35, 319–340.